Force Feedback for the Patient Side Manipulator

of the daVinci Research Kit

by

Anna Novoseltseva

A Thesis submitted to the Faculty of the

WORCESTER POLYTECHNIC INSTITUTE

in partial fulfillment of the requirements for the

Degree of Master of Science in Biomedical Engineering

Worcester, Massachusetts

May, 2018

Approved by:

_____

Prof. Gregory S. Fischer, Advisor
Worcester Polytechnic Institute

_____

Prof. Karen Troy, Committee Member
Worcester Polytechnic Institute

_____

Prof. Loris Fichera, Committee Member
Worcester Polytechnic Institute

Abstract

Teleoperated robotic surgical systems such as daVinci are widely used for laparo-scopic surgeries. The currently available daVinci system does not provide haptic feedback. Prior research has shown that the addition of haptic feedback improves surgeons' performance during minimally invasive surgeries. Other authors have implemented haptic feedback in the daVinci robot by placing sensors on the surgical tools, using visual based force estimation, and measuring proximal guide wire forces. However, they faced issues with biocompatibility, time delay, low accuracy, and repeatability.

In this work, two strain gauge based force-sensing devices were created for the patient side manipulator of the daVinci surgical robot. These devices were designed to be easily added to the existing system. The device mounted on the cannula measures the X-Y components of the forces applied to the tool, and the device mounted on the sterile adapter measures the Z-component of the force. These devices are used for the real-time force feedback in the daVinci robot.

The proposed system has high sensitivity and resolution, matches the required

force measurement range, and has high signal-to-noise ratio, which implies high signal quality. However, the absolute errors of the currently built devices are high.

This work demonstrates fast 3-DOF force measurements on the daVinci robot without any robot modifications. While the present system has significant systematic errors, these can be mitigated by altering the mechanical design to reduce hysteresis and improve the accuracy of the system.

Acknowledgments

I would like to express my gratitude to everybody in the world.

Dedication

This dissertation is dedicated to everybody in the world.

Contents

List of Tables

List of Figures

Acronyms

PSM Patient Side Manipulator

DOF Degrees of Freedom

PCB Printed Circuit Board

ROS Robot Operating System

SD Standard Deviation

SNR Signal-to-noise Ratio

Chapter 1

Introduction

Teleoperated da Vinci surgical system is a robot-assisted surgical system that enhances surgeons performance in minimally invasive surgeries by allowing highly precise translation of surgeon's hand movements to the instrument's movements.

The currently available da Vinci surgery system has a laparoscopic camera, providing visual feedback to guide doctors during surgery. However, the system does not have any kinesthetic or cutaneous feedback, known as haptics. [1]

During open surgeries, doctors usually get haptic feedback directly or through the surgical tools. In minimally invasive surgeries interaction with patients via long shafts leads to the loss of some force and tactile sense. In robotic surgery systems, surgeons have to manipulate robots indirectly, which leads to an elimination of any haptic feedback. [2]

It is believed that the addition of haptic feedback in the da Vinci surgery robot will

help to reduce the amount of surgical errors and intra-operative injuries, which will lead to faster post-surgery recovery time and decreased rate of unsuccessful surgeries. [2–4]

There are many technical challenges to overcome in order to implement the haptic feedback in da Vinci robot. One of them is getting accurate force readings from the patient side manipulator (PSM). To address this issue, we are trying to create force-feedback device, that can be easily added to the existing surgery system.

Chapter 2

Background

In this section we talk about all background knowledge necessary to

2.1 Teleoperated Surgical Robots

Recently robots started to be extensively used for surgical procedures. The use of robots allows doctors to perform surgical procedures with high accuracy, repeatability and reliability. Which in turn results in reducing operation time, errors and post-operation injuries. Minimally invasive surgeries are beneficial for accurate procedures with minimal access to operated organs, e.g. neurosurgery, eye surgery, cardiac surgery, intravascular surgeries and etc. Use of robots in minimally invasive procedures improves precision and reliabilty of operations. [**?**]

There are two types of devices used for surgeries, supporting and augmenting.

Supporting devices perform secondary functions to support the surgeon. Some of them used for positioning and stabilization purposes of cameras, endoscopic tools, ultrasound probes and etc. Others to increase device dexterity or autonomy (dexterous and autonomous endoscopes).

Augmenting devices are used to extend surgeon's ability in performing an operation. They can be divided in four categories. Hand-held tools are augmenting instruments that used for hand tremors reduction, for dexterity and navigation capability increase. Another type of augmenting devices are cooperatively-controlled tools, where the surgeon and the robot cooperatively manipulate the surgical device (e.g. ROBODOC system, Steady- Hand robot, LARS, the Neurobot, and the AC-ROBOT system). Teleoperated robots are type of augmenting tools, where surgeon (master) controls the movements of a surgical robot (slave) via a surgeon's console (e.g. the da Vinci and the Zeus systems). And autonomous tools, which can perform some tasks (suturing and knot tying) autonomously. [**?**]

Use of teleoperated robots in surgeries can solve many of the conventional surgery problems in terms of more precise manipulation capability, ergonomics, dexterity, and haptic feedback capability for the surgeon. They enhance dexterity by increase of instrument degrees of freedom, hand tremor compensation, and movements scaling that allows transformation of the control grips large movements into small motions inside the patient. 3-D view with depth perception gives surgeons ability to directly control a stable visual field with increased magnification and maneuverability. All of these

enhances the surgeon's operation performance. However, robot-assisted surgeries are high cost, need large operational room space, do not have established efficacy, and need for tableside assistants. For these reasons ability of hospitals to use surgical robots is low, making their use for routine surgeries improbable. [**?**]

Today, many surgical robotic systems have been commercially developed and approved by the FDA, such as the Da Vinci surgical system (Intuitive Surgical, Inc., Sunnyvale, CA) , Sensei X robotic catheter system (Hansen Medical Inc., Mountain View, CA), FreeHand v1.2 (FreeHand 2010 Ltd., Cardiff, UK), Invendoscopy E200 system (Invendo Medical GmbH, Germany), Flex robotic system (Medrobotics Corp., Raynham, MA), Senhance (TransEnterix, Morrisville, NC), Auris robotic endoscopy system (ARES; Auris Surgical Robotics, Silicon Valley, CA, USA), The NeoGuide Endoscopy System (NeoGuide Endoscopy System Inc, Los Gatos, CA). [**?**, **?**]

There is also number of NON-FDA-approved platforms that currently under development or going through clinical trials. For example, MiroSurge (RMC, DLR, German Aerospace Center, Oberpfaffenhofen-Weling), The ViaCath system (BIOTRONIK, Berlin, Germany), SPORT surgical system (Titan Medical Inc., Toronto, Ontario), The SurgiBot (TransEnterix, Morrisville, NC), The Versius Robotic System (Cambridge Medical Robotics Ltd., Cambridge, UK), MASTER (Nanyang Technological University and National University Health System), Verb Surgical (Verb Surgical Inc., J & J/Alphabet, Mountain View, CA, USA), Miniature in vivo robot (MIVR) (MIVR, Virtual Incision, CAST, University of Nebraska Medical Center, Omaha,

Nebraska, USA), the Einstein surgical robot (Medtronic, Minneapolis, MN). [**?**]

The da Vinci Surgical System is one of the most commonly used robotic surgical systems. In 2015, over 3400 systems were in use around the world. More than 3 million surgeries were performed worldwide using da Vinci system [1]. The system has been approved for various types of surgeries such as cardiac, colorectal, thoracic, urological and gynecologic. However, new systems are emerging on the market, providing features that are absent currently in the da Vinci System. For example, in 2017 FDA approved Senhance robotic platform that provides actual haptic force feedback, allowing the surgeon to feel forces generated at the instruments end. In addition, the system uses eye-tracking technology to move the camera at the point the surgeon is looking at, while the da Vinci uses a footswitch panel to control the camera movement. Another example is Flex Robotic System, which consists of flexible endoscope for laparoendoscopic surgeries. This system is able to define a non-linear path to surgical target by advancing a flexible telescopic inner-outer mechanism with instruments inside it, whereas instruments in the da Vinci system can follow only non-flexible straight path. [**?**]

Effectiveness of da Vinci system in comparison to opened surgery and other systems [5]

2.2　Importance of Haptic Feedback

Write about studies with and without haptic feedback.

It has been shown that incorporating force feedback into teleoperated sys- tems can reduce the magnitude of contact forces and therefore the energy consumption, the task completion time and the number of errors. In sev- eral studies [122, 147, 15], addition of force feedback is reported to achieve some or all of the following: reduction of the RMS force by 30

In [106], a scenario is proposed to incorporate force feedback into the Zeus surgical system by integrating a PHANToM haptic input device into the system. In [85], a dextrous slave combined with a modified PHAN- ToM haptic master which is capable of haptic feedback in four DOFs is presented. A slave system which uses a modified Impulse Engine as the haptic master device is described in [30]. In [107], a telesurgery master- slave system that is capable of reflecting forces in three degrees of freedom (DOFs) is discussed. A master-slave system composed of a 6-DOF parallel slave micromanipulator and a 6-DOF parallel haptic master manipulator is described in [150]. Other examples of haptic surgical teleoperation include [93] and [11]. The haptics technology can also be used for surgical training and simulation purposes. For example, a 7-DOF haptic device that can be applied to surgical training is developed in [56]. A 5-DOF haptic mecha- nism that is used as part of a training simulator for urological operations is discussed in [146].

2.3 Current Approaches

1.3 Haptics for Robotic Surgery and Therapy Incorporating haptic sensation to robotic systems for surgery or therapy especially for minimally invasive surgery, which involves limited instrument maneuverability and 2-D camera vision, is a logical next step in the develop- ment of these systems. To do so, in addition to instrumentation of surgical tools, appropriate haptics-enabled user interfaces must be developed.

1.3.1 Haptic user interface technology In the following, examples of the currently available haptic devices are described. For a more complete survey of haptic devices, see [55].

1.3.1.1 PHANToM The PHANToM from Sensable Technologies Inc. (www.sensable.com) is one of the most commonly used haptic devices and comes in a number of models with different features. PHANToM 1.5A provides six DOFs input control. Of the six DOFs of the arm, depending on the model, some or all are force-reflective. In Figure 1.2a, a PHANToM 1.5/6DOF with force feedback capability in all of the six DOFs is shown.

1.3.1.2 Freedom-6S The Freedom-6S shown in Figure 1.2b is a 6-DOF device from MPB Technologies Inc. (www.mpb-technologies.ca) that provides force feedback in all of the six degrees of freedom. The position stage is direct driven while the orientation stage is driven remotely by tendons. The Freedom-6S features static and dynamic balancing in all axes (see [54] for further design details). 1.3.1.3 Laparoscopic Impulse Engine and Surgical Workstation Originally as part of a laparoscopic

surgical simulator, the Laparoscopic Impulse Engine was designed by Immersion Corp. (www.immersion.com). The device can track the position of the instrument tip in five DOFs with high resolution and speed while providing force feedback in three DOFs. More recently, Immersion has developed the Laparoscopic Surgical Work-station (Figure 1.2c), which is capable of providing force feedback in five DOFs. An application example is the Virtual Endoscopic Surgery Trainer (VEST) from Select-IT VEST Systems AG (www.select-it.de). The VEST system uses the Laparoscopic Impulse Engine as its force-feedback input interface for simulating laparoscopic surgery interventions.

1.3.1.4 Xitact IHP The Xitact IHPTM from Xitact Medical Simulation (www.xitact.com) is a 4-DOF force feedback manipulator based on a spherical remote-center-of- motion mechanical structure and was originally designed for virtual reality based minimally invasive surgery simulation [42]. It features high output force capability, low friction, zero backlash and a large, singularity-free workspace. A picture of the Xitact IHP is shown in Figure 1.2d.

Placing force sensors on the surgical instrument [6]

They suggest to the measure of pulling and grasp forces at the tip of surgical instrument. For the design of the compliant forceps, the required compliance charac-teristics are first defined using a simple spring model with one linear and one torsional springs. This model may be directly realized as the compliant forceps. However, for the compact realization of the mechanism, we synthesize the spring model with two

torsional springs that has equivalent compliance characteristics to the linear-torsional spring model. Then, each of the synthesized torsional springs is realized physically by means of a flexure hinge. From this design approach, direct measurement of the pulling and grasp forces is possible at the forceps, and measuring sensitivity can be adjusted in the synthesis process. The validity of the design is evaluated by finite element analysis. Further, from the measured values of bending strains of two flexure hinges, a method to compute the decoupled pulling and grasp forces is presented via the theory of screws. Finally, force- sensing performance of the proposed compliant forceps is verified from the experiments of the prototype using some weights and load cells. 10.1109/TRO.2012.2194889

Making new surgical instrument design [7]

Method In this paper a force-feedback enabled surgical robotic system is described in which the developed force-sensing surgical tool is discussed in detail. The developed surgical tool makes use of a proximally located force/torque sensor, which, in contrast to a distally located sensor, requires no miniaturization or sterilizability. Results Experimental results are presented, and indicate high force sensing accuracies with errors ¡0.09 N. Conclusions It is shown that developing a force-sensing surgical tool utilizing a proximally located force/torque sensor is feasible, where a tool outer diameter of 12 mm can be achieved. For future work it is desired to decrease the current tool outer diameter to 10 mm.

Sensorless estimation methods

Vision based solution [8]

They proposed to use vision based solution with supervised learning to estimate the applied force and provide the surgeon with a suitable representation of it. The proposed solution starts with extracting the geometry of motion of the heart's surface by minimizing an energy functional to recover its 3D deformable structure. A deep network, based on a LSTM-RNN architecture, is then used to learn the relationship between the extracted visual-geometric information and the applied force, and to find accurate mapping between the two. Our proposed force estimation solution avoids the drawbacks usually associated with force sensing devices, such as biocompatibility and integration issues. We evaluate our approach on phantom and realistic tissues in which we report an average root-mean square error of 0.02 N.

SLiding pertrubation observer

This paper suggests a bilateral controller applying sliding perturbation observer based force estimation method. In the suggested bilateral controller, the master control uses impedance control and the slave control uses a sliding mode control (SMC). A torque and force sensorless teleoperation system can be implemented using the suggested bilateral control structure through an experimental evaluation. This paper presents a method of estimating the reaction force of the surgical robot instrument without sensors and attempts to use state observer of control algorithm. Sliding mode control with sliding perturbation observer (SMCSPO) is used to drive the instrument, where the sliding perturbation observer (SPO) computes the amount of perturbation

defined as the combination of the uncertainties and nonlinear terms where the major uncertainties arise from the reaction force. Based on this idea, this paper proposes a method to estimate the reaction force on the end-effector tip of the surgical robot instruments using only SPO and encoder without any additional sensors. To evaluate the validity of this paper, experiment was performed and the results showed that the estimated force computed from SPO is similar to the actual force.

Measuring the proximal guide wire force [9]

They measure the proximal guide wire force and the force between the surgeon's hand and the handle used on the Phantom, the force feedback closed-loop control can effectively eliminate the loss of mechanical impedance of force feedback information. The accuracy control of force feedback is greatly enhanced in the aspect of security and the operation efficiency.

Write about all disadvantages of previous methods.

Tools - ¿limited lifetime - find citation

Vision -¿ huge time delays, accuracy

Wire force - ¿ repeatability issue

2.4   Force Sensors

Two general principles dominate in force measurement: piezoelectric and strain-gauge sensors. [10]

Piezoelectric sensors consist of two crystal disks with an electrode foil in between. When force is applied, an electric charge, proportional to the applied force, is obtained and can be measured. Piezoelectric sensors show small deformation when force is applied, this results in a high resonance frequency. Also, piezoelectric sensors due to their principle of operation have significant linearity error and drift. [11]

In the strain gauge based force transducers the force causes deformation and subsequent linear change in resistance. Strain gauges are usually connected to a Wheatstone bridge circuit, where the output voltage is proportional to the applied force. Strain gauge based transducers provide small individual errors (200 ppm), show no drift, and are therefore appropriate for long-term monitoring tasks. However, they are relatively big, temperature dependent, and have lower resonance frequency in comparison to piezoelectric sensors. [10, 11]

On the basis of the above mentioned, piezoelectric sensors are preferable for dynamic measurements of small forces while strain gauge sensors are better when large forces are measured. In this study, strain gauges were used since they show better accuracy and long-term stability. [10, 11]

We can use QTC-pills, but it has no-linearity and hysteresis issues. We can test in the future.

2.5 Contributions

Force sensing devices for measuring forces in X-Y direction and one for Z-direction measurement were created. They allow to get accurate force readings from the da Vinci tools of the PSM. These devices can be easily added to the existing da Vinci system. Since we have to add created device on each robot arm only, it is cheaper than placement of sensors on each separate surgical tool. Moreover, created devices allow to get force data faster than through visual data processing method.

Chapter 3

Methods and Results

3.1   Force Measurement

Block diagram of the created system for 3-DOF force measurement is shown on figure 3.1. Forces that applied on the end of surgical tool are measured using strain gauges, which change their resistance with force. Using created printed circuit boards (PCBs), this resistance changes are measured and published within ROS. At the same time we measure current joint position of the tool, which is needed for the force calibration. On the PC position data and data from PCBs are used to find values of the force in X,Y,Z directions.
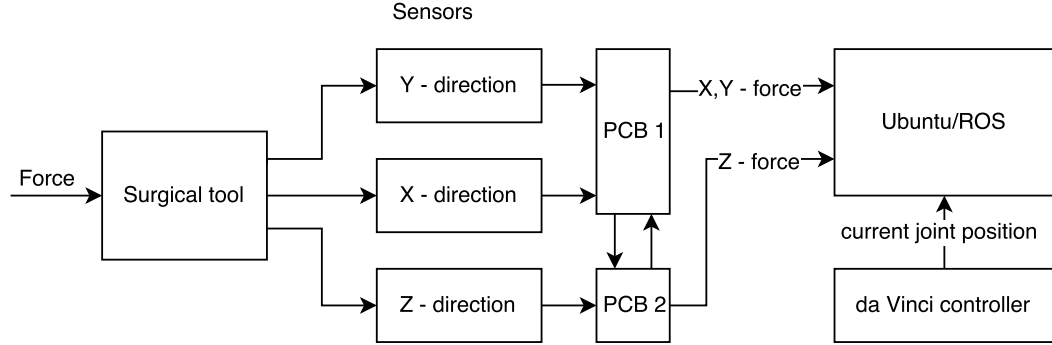
Figure 3.1: Block diagram

3.2 Sensor Placement Optimization

A finite element analysis was done in Solidworks to assess better placement of the strain gauges on the created device. In order to run finite element analysis material properties, such as elastic modulus, poisson's ratio, and density are necessary to know. Sleeve material is aluminum 6061, that has elastic modulus 68.9 GPa, poisson's ratio 0.33, and density 2700 kg/m^3 [**?**]. Since the shaft and cannula materials are unknown, in order to run finite element analysis their elasticity modulus and density were found experimentally.

3.2.1 Elastic Modulus Measurements

Elastic Modulus of the shaft and the cannula were found experimentally (Figure 3.2). One end of the observing sample (shaft/cannula) was fixed and the force was applied on the other end. We used weights 250g for the shaft and 555g for the cannula to apply forces. The deformation caused by forces was detected with dial indicator.

Table 3.1: Elasticity Modulus Measurement Data

Component	d_o, mm	d_i, mm	I, mm^4	m, g	F, N	L, mm	L_{tot}, mm
Shaft	8.4	6	$1.808 \cdot 10^{-10}$	250	3.25	276.2	366.8
Cannula	10.54	8.75	$3.181 \cdot 10^{-10}$	555	6.011	95.5	105.55

Component	$\delta \pm SD$, mm	$E \pm SD$, GPa
Shaft	2.856 ± 0.123	44.31 ± 1.86
Cannula	0.086 ± 0.004	63.92 ± 2.97

Experiment was done 5 times, average displacement value was used to calculate elastic modulus. Results are shown in Table 3.1.
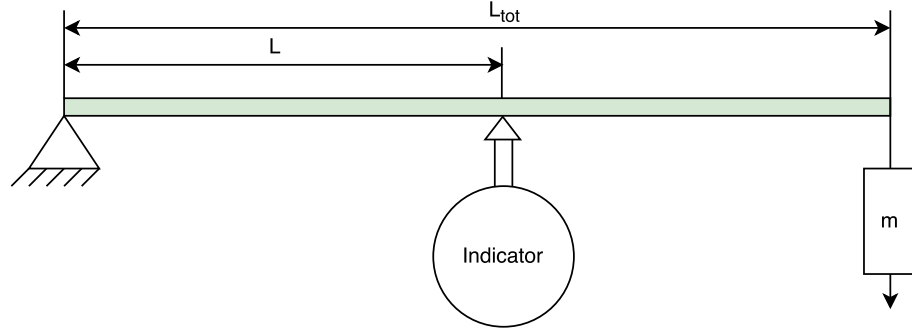

Figure 3.2: Setup to measure elasticity modulus

Elastic Modulus was found using following equation:

$$E = \frac{FL^3}{3\delta I} \tag{3.1}$$

where F - force, L - length from the fixed point to indicator, I - area moment of inertia, δ - displacement.

Area moment of Inertia:

$$I = \frac{\pi(d_o^4 - d_i^4)}{64} \tag{3.2}$$

where d_o - cylinder outside diameter, d_i - cylinder inside diameter.

17

Force acting on indicator:

$$F = \frac{L_{tot}}{L} mg \qquad (3.3)$$

where L_{tot} - total length of the object, m - mass of the weight, g - gravitational constant.

Experimentally found mean value of elastic modulus of the shaft is equal to 44.31 GPa with standard deviation (SD) 1.86 GPa, elastic modulus of the cannula is 63.92 GPa with SD 2.97 GPa, which is close to aluminum modulus of elasticity (68.9 GPa [?]).

3.2.2 Density Measurements

Density was found using following equation:

$$p = \frac{m}{V} \qquad (3.4)$$

where m - mass, V - volume.

Shaft material density is 3380 kg/m^3. From the elastic modulus of the cannula, we assumed that it is made of aluminum and consequently has density equal to 2700 kg/ m^3.

Table 3.2: Material Properties

Component	Elastic Modulus, GPa	Density, kg/ m^3
Shaft	44.31	3380
Cannula	63.92	2700
Sleeve	68.9	2700

3.2.3 Simulation Results

From the Figure 2, it can be seen that the mounting location of the cannula seems to be under the greatest amount of strain. Additionally, the slight gap between the cannula and the DaVinci tool creates a large load point at the tip of the cannula as well as creating a slight moment of inaccuracy in readings at small loads.

We suggest to place strain gauges at the mounting location of the cannula. Maximum strain is 0.46 mm, in case of 10N load with maximally opened shaft. From the literature, strain gauges length should be more than 5

Gauge Factor (GF) for strain gauges usually is 2. According to the formula (4) strain gauge with resistance 120 will give change in resistance 0.115 , and 350 - 0.338 : R=GFR, where GF - gauge factor, R - resistance, - strain.

All material properties are listed in Table 3.2.

3.3   Requirements for the Device

From the literature review, following requiremetns for the device were developed:

Biocompatibility

Linearity

Range of forces Highest gripping force in Da Vinci tool was seen in the Hemo-lok[R] clip applier (39.92 [+ or -] 0.89 N). 0.3 - 11 N. Tensile strength and failure load of sutures for robotic surgery Others

3.4 Mechanical Design

At first we were rying to put sensors on the instrument shaft itself, on the cannula, on the sleeve to see where we get the most accurate results.

3.4.1 Strain Gauge

According to the manual for strain gauge selection provided by Vishay Micro-Measurements. The strain gauge should have following parameters: Gauge length is 0.8 mm. Ideally gauge length should be 10 % of the shaft radius; Single grid; Isoelastic (D alloy) that has higher gauge factor with E backing; Encapsulated with pre attached leads; Resistance 120 Ohms; Gauge factor - 2; STC number (self-temperature-compensation): DY dynamic Since the diameter of the shaft is only 8.5 mm, one of the most important parameters, in this case, is the size of the strain gauge. Another important parameter is gauges resistance, sensitivity of the strain gauge drastically depends on this parameter. Strain gauges with different resistivity were used (350 and 120 Ohms and sizes of 6 x 2.5 mm).

3.4.2   Installation of Strain Gauges

The shaft was assumed to be made of Tecamax, but for gauge installation purposes materials for plastic was chosen as it is comparable in preparation. [12].

First the working surface (glass) and tweezers were cleaned with Neutralizer 5. After that shaft surface preparation was started, using solvent degreaser GC-6 Isopropyl Alcohol. A gauge layout was then applied with a 4H drafting pencil. The surface was then conditioned with Conditioner A and the extra liquid was wiped with gauze. Finally, the surface was then neutralized with M-Prep Neutralizer 5A. [12]

The strain gauges were first placed on the glass and then transported using mylar tape onto the instrument surface. A thin layer of catalyst was applied on the strain gauge and given one minute to dry. Then adhesive M-BOND 200 was applied on the shaft, pressure was applied on the tape for one minute, then two more minutes to let it dry before the tape was removed. Then leads soldering was done by application of pats, and soldering them with thin wires. [13]

The methodology of the strain gauge application more specifically described in [12].

In compliance with the literature [12] for application of the strain gauge on metals, the same materials and technique can be used. Therefore, the same method to apply strain gauges on the cannula was used.

On the shaft On the cannula On the aluminum sleeve On the nylon sleeve
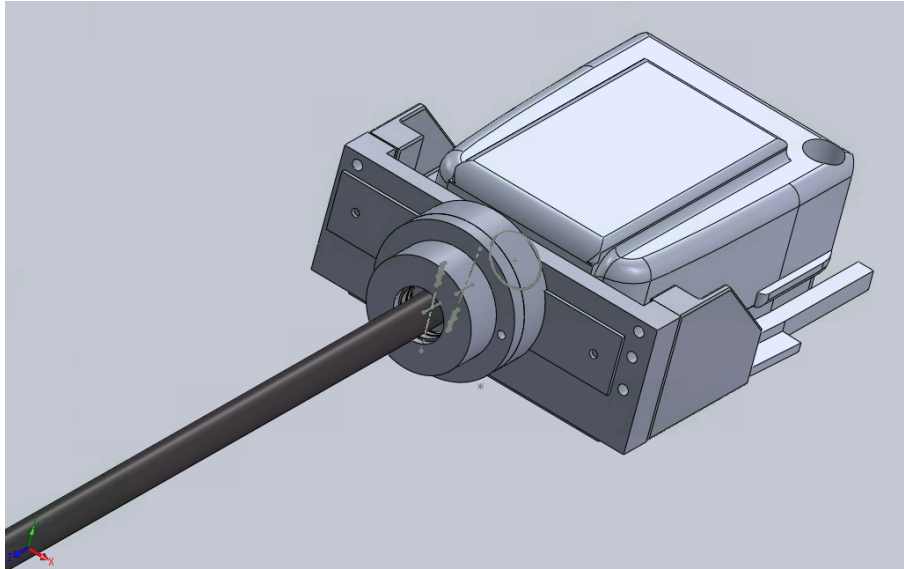
Figure 3.3: Z-direction force feedback sensor

3.4.3   Sensors on the tool and the cannula

3.4.4   X-Y direction

Do not use 3D printed sleeves - causes non-linearity issue Use 350 Ohm strain-gauges and full-bridge circuit.

3.4.5   Z-direction

3.5   Electrical and Software Design

Using Altium Designer 15.1 PCB was developed and manufactured elsewhere.

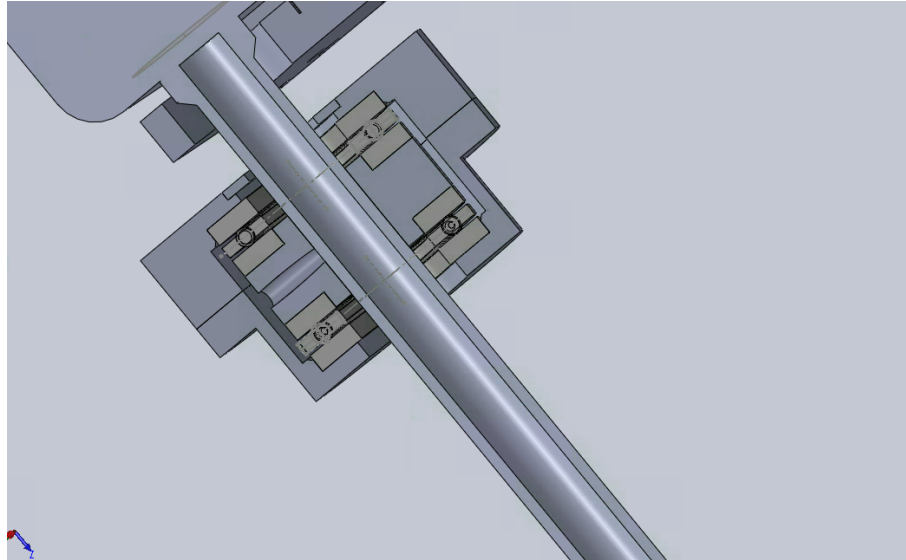Write about how to calibrate the PCB itself and how it works.

Figure 3.4: Z-direction force feedback sensor - section vew

3.5.1   Circuit design

Write about how circuit works.

3.5.2   Noise Analysis

Noise analysis was performed using oscilloscope ... Make FFT analysis

3.5.3   Microcontroller Software

We use arduino for .. Filtering was implemented on microcontroller by finding average of recent 5 readings Filtering - ideally small time delay. Total teleoperation cycle delay - less than 100ms (visually noticeable delay). Kalman filter? Use same parameters for both signals to get identical time delay. good article about changing
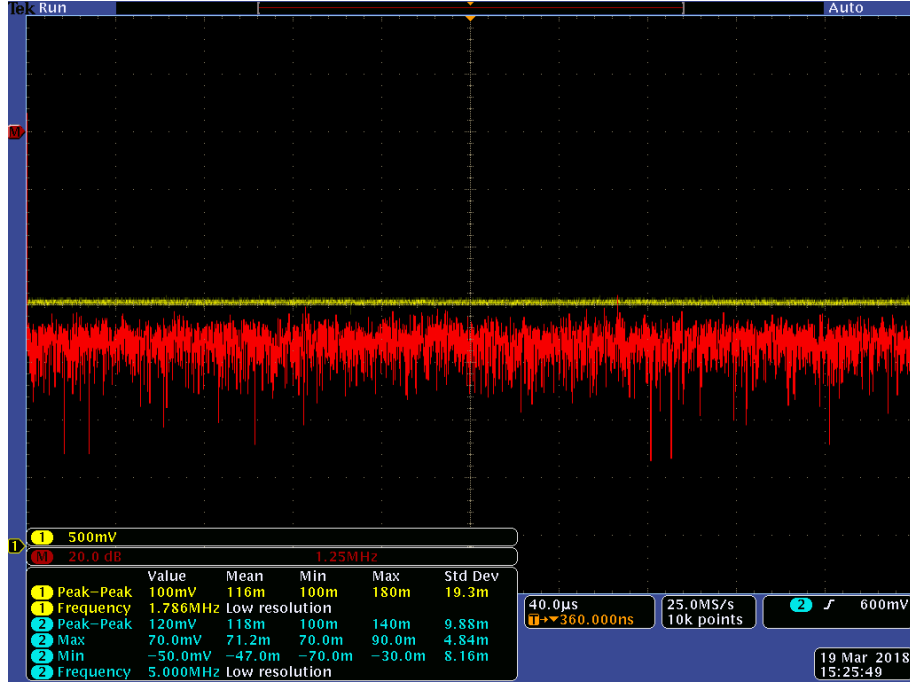
Figure 3.5: Noise analysis of the output signal

baud rate.

3.5.4 ROS Architecture

3.6 Calibration

First we used set of weights applied in two directions, but since the system was too sensitive for direction of force, we had to change our approach of determining the force direction. It was decided to use optical tracking system for that purpose.

3.6.1   Calibration Setup

Tell how calibration with optical tracking system is working

3.6.2   Calibration of the Load Cell

Was peformed using following setup cite figure .. Calibration equation we got ..

3.6.3   Calibration Results

Find mean square root error

3.7   Experiments

3.7.1   Distance from the cannula to the tip dependence from readings

Distance from the cannula to the tip - measure - 3 inch. Maximum distance is 9 inches.

3.7.2   Temeperature Dependence

Try in 36.6 Celsius and room temperature Effect of the surrounding temperature on the device was ..
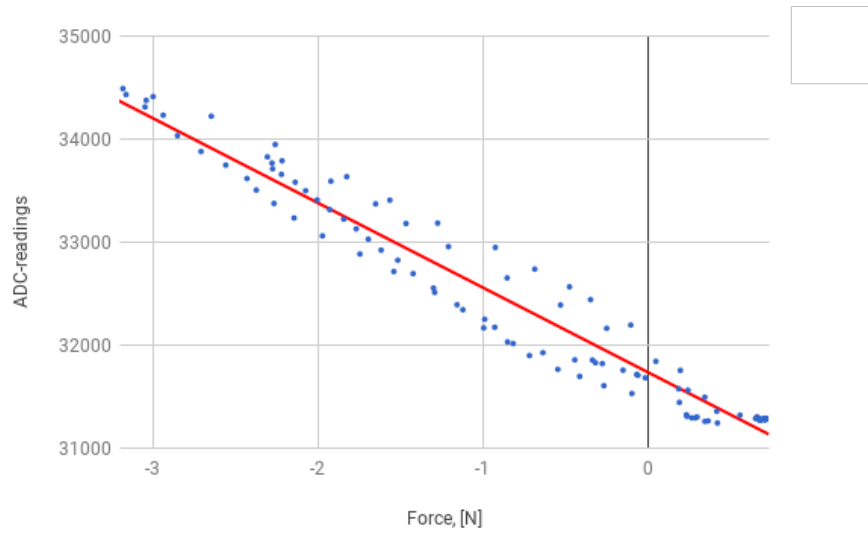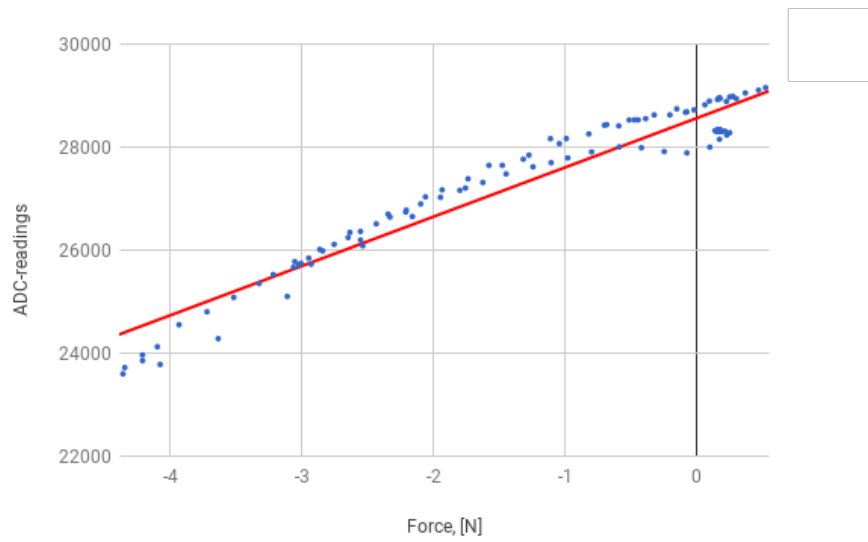
Figure 3.6: X-component

Figure 3.7: Y-component

Figure 3.8: Calibration results

Do all experiments at least three times and calculate all statistic things you can (SD)

3.7.3 Hysteresis

Hysteresis was checked .. We written separate program to check hysteresis

3.7.4 Static Characteristics

Precision represents capacity of a sensing system to give the same reading when repetitively measuring the same measurand under the same conditions. The precision is a statistical parameter and can be assessed by the standard deviation (or variance) of a set of readings of the system for similar inputs.

One of the measurements of signal quality is signal-to-noise ratio (SNR). A higher value of SNR means the clear acquisitions with low signal distortions and artifacts caused by unwanted noise. It is defined as:

$$\frac{S}{N} = \frac{Meanvalueofsignal}{Standarddeviationofnoise} \tag{3.5}$$

For X-direction SNR is 3232 ± 78, for Y-direction SNR is 2857 ± 150, which is much bigger than 1. It means that system has very low noise.

Error is the difference between the actual value of the measurand and the value produced by the sensing system. Error can be caused by a variety of internal and
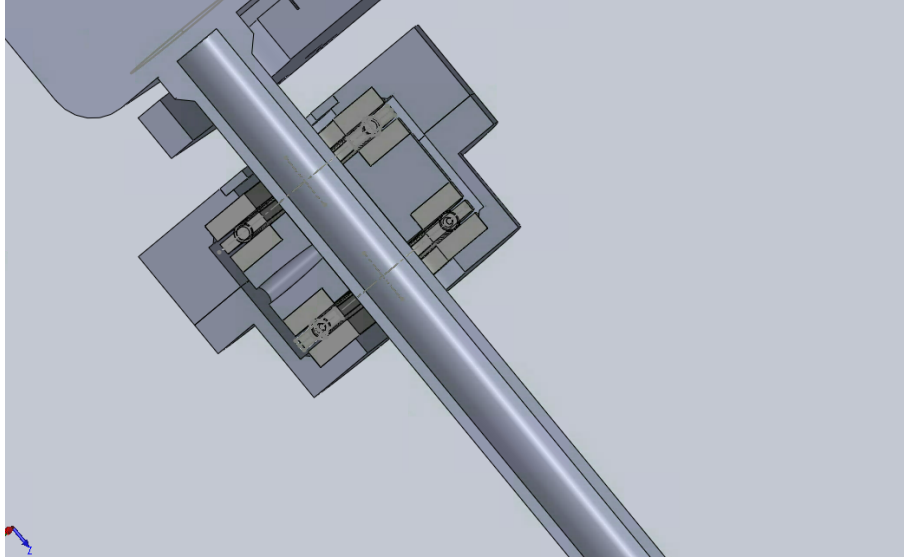
Figure 3.9: Z-direction force feedback sensor - section vew

external sources and is closely related to accuracy. Accuracy can be related to absolute

or relative error as:

$$Absolute error = \frac{Output}{True value} \tag{3.6}$$

From figure we can assume that fluctuations in the output signal are due to

systematic errors.

Drift is observed when a gradual change in the sensing systems output is seen,

while the measurand actually remains constant. Drift is the undesired change that

is unrelated to the measurand. It is considered a systematic error, which can be

attributed to interfering parameters such as mechanical instability and temperature

instability, contamination, and the sensors materials degradation.

Resolution (or discrimination) is the minimal change of the measurand that can

produce a detectable increment in the output signal. Resolution is strongly limited by any noise in the signal.

In a sensing system, minimum detectable signal (MDS) is the minimum signal increment that can be observed, when all interfering factors are taken into account. When the increment is assessed from zero, the value is generally referred to as threshold or detection limit. If the interferences are large relative to the input, it will be difficult to extract a clear signal and a small MDS cannot be obtained.

Sensitivity is the ratio of the incremental change in the sensors output (Dy) to the incremental change of the measurand in input (Dx). The slope of the calibration curve, y f(x), can be used for the calculation of sensitivity.

The closeness of the calibration curve to a specified straight line shows the linearity of a sensor. Its degree of resemblance to a straight line describes how linear a system is.

Hysteresis is the difference between output readings for the same measurand, depending on the trajectory followed by the sensor.

The maximum and minimum values of the measurand that can be measured with a sensing system are called the measurement range, which is also called the dynamic range or span. This range results in a meaningful and accurate output for the sensing system. [?]

Chapter 4

Discussion and Conclusion

Compare shaft, cannula, sleeve - accuracy, hysteresis.

This is our conclusion)

For future work .. However, disadvantages would be addition of the cost to already expensive system and possible biocompaitibily and sterilization issues. Also addition of the weight to the arm could alter robot performance, however, since the device will be placed close to center of rotation of the robot arm, it will have minimal affect on the moment of inertia in comparison to sensors added to the grippers.

Bio-compatibility and coatings

Sterilization techniques

Z-direction. We tried to measure force in Z-direction, but unfortunately results shown that developed system was not accurate and sensitive enough. To improve system we can suggest to change strain gauges to more sensitive ones. Since we have

small room for deformation - around 0.3 mm, we can not afford more deformation by using thinner or longer plates. Therefore, we decided to use motor current readings for z-directional reading of the force.

Increase speed form 588 Hz to something higher by change ADC from SPI communication to parallel communication. Right now maximum frequency is 250ksps, which is $250k/32 = 7.812$ KBps.

Change communication channel bw microcontroller and PC to faster one. Right now we use serial port, with max speed 7.1 KBps

Change microcontroller to the faster one.

We can use QTC-pills in future, promising approach, higher sensitivity

References

[1] Intuitive surgical, inc. - da vinci surgical system. [Online]. Available: https://www.intuitivesurgical.com/

[2] A. M. Okamura, "Haptic feedback in robot-assisted minimally invasive surgery," vol. 19, no. 1, pp. 102–107.

[3] C. E. Reiley, T. Akinbiyi, D. Burschka, D. C. Chang, A. M. Okamura, and D. D. Yuh, "Effects of visual force feedback on robot-assisted surgical task performance," vol. 135, no. 1, pp. 196–202.

[4] O. A. J. van der Meijden and M. P. Schijven, "The value of haptic feedback in conventional and robot-assisted minimal invasive surgery and virtual reality training: a current review," vol. 23, no. 6, pp. 1180–1190.

[5] J. Yu, Y. Wang, Y. Li, X. Li, C. Li, and J. Shen, "The safety and effectiveness of da vinci surgical system compared with open surgery and laparoscopic surgery: a rapid assessment," vol. 7, no. 2, pp. 121–134.

[6] M. B. Hong and Y. H. Jo, "Design and evaluation of 2-DOF compliant forceps with force-sensing capability for minimally invasive robot surgery," vol. 28, no. 4, pp. 932–941.

[7] W. Schwalb, B. Shirinzadeh, and J. Smith, "A forcesensing surgical tool with a proximally located force/torque sensor," vol. 13, no. 1.

[8] A. I. Aviles, S. M. Alsaleh, J. K. Hahn, and A. Casals, "Towards retrieving force feedback in robotic-assisted surgery: A supervised neuro-recurrent-vision approach," vol. 10, no. 3, pp. 431–443.

[9] S. M. Yoon, W. J. Kim, and M. C. Lee, "Design of bilateral control for force feedback in surgical robot," vol. 13, no. 4, pp. 916–925.

[10] HBM. (2017) Piezoelectric or Strain Gauge Based Force Transducers? [Online]. Available: https://www.hbm.com/en/3719/piezoelectric-or-strain-gauge-based-force-transducers/

[11] A. sensors. (2017) Piezoelectric Sensors and Strain Gauge-based Force Transducers: Principles in Force Measurement. [Online]. Available: http://www.azosensors.com/article.aspx?ArticleID=281

[12] MICRO-MEASUREMENTS. (2014) Surface Preparation for Strain Gage Bonding. [Online]. Available: http://www.vishaypg.com/docs/11129/11129B129.pdf

[13] V. P. Group. Cea Strain Gage Installation with M-Bond 200 Adhesive (Training Video) - Micro-Measurements. Youtube. [Online]. Available: https://www.youtube.com/watch?v=SjXpF61HRys